

4-1-2016

The potential role of polyamines in gill epithelial remodeling during extreme hypoosmotic challenges in the Gulf killifish, *Fundulus grandis*

Ying Guan
Louisiana State University

Guo xia Zhang
Southern Medical University

Shujun Zhang
Louisiana State University

Beau Domangue
Louisiana State University

Fernando Galvez
Louisiana State University

Follow this and additional works at: https://digitalcommons.lsu.edu/biosci_pubs

Recommended Citation

Guan, Y., Zhang, G., Zhang, S., Domangue, B., & Galvez, F. (2016). The potential role of polyamines in gill epithelial remodeling during extreme hypoosmotic challenges in the Gulf killifish, *Fundulus grandis*. *Comparative Biochemistry and Physiology Part - B: Biochemistry and Molecular Biology*, 194-195, 39-50. <https://doi.org/10.1016/j.cbpb.2016.01.003>

This Article is brought to you for free and open access by the Department of Biological Sciences at LSU Digital Commons. It has been accepted for inclusion in Faculty Publications by an authorized administrator of LSU Digital Commons. For more information, please contact ir@lsu.edu.

1 **ABSTRACT**

2 Polyamines are a family of low molecular weight organic cations produced in part by the
3 coordinated actions of arginase II (Arg II) and ornithine decarboxylase (Odc). Although gill
4 polyamine homeostasis is affected by acute transfer to fresh water, little is known of its function
5 in fish osmoregulation. The current study investigated the role of polyamines in the
6 compensatory response of hypoosmotic challenge in the euryhaline fish, *Fundulus grandis*.
7 Adult *F. grandis* were acclimated to 5 ppt water, transferred abruptly to 5, 2, 1, 0.5 and 0.1 ppt
8 water, and assessed for osmoregulatory function, gill morphology, and polyamine homeostasis.
9 The plasma osmolality, Na⁺ concentration, and Cl⁻ concentration were only significantly reduced
10 during exposure to salinities at or below 0.5 ppt, although these effects were transient except in
11 the 0.1 ppt treatment. The phenotype of mitochondrion-rich cells (MRCs) shifted from a
12 seawater-type to a freshwater-type only at salinities that also produced a plasma osmotic
13 disturbance. Hypoosmotic exposure increased the concentrations of putrescine, spermidine, and
14 spermine in the gill over the entire 7 day period. Exposure to 0.1 ppt water also transiently
15 increased gill caspase-3 activity and gill mRNA levels of the immediate-early response genes, *c-*
16 *fos* and *c-myc*, thus tightly associating polyamines with gill remodeling during freshwater
17 acclimation. Furthermore, arginase II and ornithine decarboxylase mRNA levels were most
18 highly expressed in MRCs, and these levels were further increased only in the 0.1 ppt treatment.
19 Reduction of gill polyamine levels following administration of the Odc inhibitor, alpha-DL-
20 difluoromethylornithine (DFMO), inhibited gill caspase-3 activity, but surprisingly reduced the
21 magnitude of the plasma osmotic imbalance elicited by exposure to 0.1 ppt water. We used
22 isolated opercular epithelia mounted on Ussing chambers to assess the influence of polyamines
23 on the attenuating response of hypotonic shock on active Cl⁻ secretion. Spermidine partially
24 reduced the decrease of short-circuit current (I_{sc}) and membrane conductance (G_t) produced by
25 hypotonic exposure. These data suggest polyamines blunt the hypotonic inhibition of NaCl
26 secretion and may lead to early apoptosis of seawater ionocytes and their replacement by FW-
27 type ionocytes.

28 Key words: Cell volume regulation; Apoptosis; Cell signaling; Ionocytes; Polyamines

29 ¹Abbreviations

¹ Abbreviations: Arg II, arginase II; DFMO, alpha-DL-difluoromethylornithine; ESTs, expressed sequence tags; FW, freshwater; G_t , membrane conductance; Hypo, hypotonic; I_{sc} , short-circuit current; Iso, isotonic; MRCs, mitochondrion-rich cells; Odc, ornithine decarboxylase; PBS, phosphate-buffered saline; PUT, putrescine; PVCs, pavement cells; SEM, scanning electron microscopic; SP, spermine; SPD, spermidine; SW, seawater

30 **Introduction**

31

32 The Gulf killifish, *Fundulus grandis*, and its sister taxa, *Fundulus heteroclitus*, reside in
33 coastal marshes that are subject to frequent and episodic oscillations in salinity, dissolved oxygen,
34 and temperature (Marshall, 2003; Wood and LeMoigne, 1991). The ability of these species to
35 tolerate dynamic habitats has made them a widely accepted model for studying the physiological
36 basis of tolerance to environmental stressors (Burnett et al., 2007). Although they prefer
37 brackish to marine environments (Kaneko and Katoh, 2004; Wood and Grosell, 2008),
38 euryhaline *Fundulus* species can cope with reduced environmental salinity and can take short
39 forays into fresh water for feeding (Marshall, 2003). Killifish appear to tolerate these short bouts
40 of fresh water by making rapid, yet easily reversible physiological adjustments (Kaneko and
41 Katoh, 2004; Wood and Grosell, 2008). Only with prolonged exposure to fresh water do they
42 make more substantial compensatory adjustments in the physiology of their ion-transporting
43 epithelia (Scott et al., 2004; Whitehead et al., 2011a; Whitehead et al., 2011b; Whitehead et al.,
44 2012; Wood and Grosell, 2008).

45 The fish gill, which consists of several cell types that mediate the active excretion of salts in
46 marine fish and the active uptake of osmolytes in freshwater fish, is critical to whole animal
47 osmoregulation (Evans et al., 2005). The gill epithelium has the ability to remodel itself in
48 response to environmental and physiological perturbations (Evans et al., 2005); however, few
49 studies have delineated the salinity at which the gill epithelium transitions from a seawater (SW)
50 to a freshwater (FW) morphology (Katoh and Kaneko, 2003; Laurent et al., 2006). Most
51 *Fundulus* species are marine teleosts that have the ability to retain their seawater physiology at
52 salinities approaching fresh water (Copeland, 1950; Griffith, 1974). *Fundulus heteroclitus* make
53 this physiological transition at a salinity between 2 ppt and 0.2 ppt based on a morphological
54 assessment of the cell types on the fish gill surface in the days following hypoosmotic challenge
55 (Copeland, 1950). Wood and Grosell (2009) report that the transepithelial potential, an
56 important determinant of the electrochemical driving force of gill ion transport, reverses in
57 polarity instantaneously following acute transfer of SW-acclimated *F. heteroclitus* to fresh water.
58 Only with prolonged exposure to fresh water do the gills of *F. heteroclitus* functionally “switch”
59 into one characteristic of a freshwater fish (Wood and Grosell, 2008, 2009). Recently, it has
60 been shown that *F. heteroclitus* acclimated to sea water can be transferred abruptly to 0.4 ppt

61 with no significant effects to their plasma osmolality and osmolyte concentrations over the 14 d
62 post-transfer (Whitehead et al., 2012). Although the ability of the gill to remodel with varying
63 environmental salinities is well reported, few investigations have described the cellular
64 mechanisms regulating the transient and long term responses of the fish gill to osmotic
65 challenges.

66 Our group has recently shown that the up-regulation of gill mRNA transcripts associated
67 with polyamine biosynthesis is amongst the most highly upregulated responses of *F. heteroclitus*
68 to hypoosmotic exposure. Furthermore, these transcriptomic responses are most pronounced
69 when the physiological compensation to the hypoosmotic exposure is initiated (Whitehead et al.,
70 2011a). Polyamines are a family of organic cations in cells, and their synthesis is affected by
71 environmental salinity in bacteria (Peter et al., 1978), plants (Zapata et al., 2004) and mammalian
72 cells (Poulin et al., 1991). Polyamines, which include the putrescine, spermidine and spermine,
73 are all increased in the killifish gill during extreme hypoosmotic challenge; a response including
74 an increased transcription and enzyme activity of ornithine decarboxylase, the first and rate-
75 limiting step converting ornithine to putrescine. Following 3 days of acute transfer from sea
76 water to fresh water, only gill putrescine remained elevated in concentration in killifish either
77 due to the increased synthesis from ornithine, reconversion of spermine/spermidine back into
78 putrescine, or due to decreased catabolism. Regardless, these data indicate there may be a
79 distinct role of this polyamine in freshwater acclimation and potentially in the maintenance of the
80 freshwater gill phenotype. Despite this information, little is known about the physiological
81 function of these molecules in fish.

82 The main goals of this study were to characterize the possible roles of ornithine
83 decarboxylase and polyamines in whole-animal osmoregulation and gill remodeling in Gulf
84 killifish during exposure to a highly-resolved range of low environmental salinities. A series of
85 exposures to low environmental salinities were performed to assess the transition between the
86 marine and freshwater gill phenotype as characterized by assessment of differences in the apical
87 opening of mitochondrion-rich cells on the fish gill surface. These findings were also
88 corroborated with plasma osmolality and markers of apoptosis during acclimation to
89 hypoosmotic challenges. We then studied the influence of alpha-DL-difluoromethylornithine
90 (DFMO), an irreversible inhibitor of ornithine decarboxylase, on plasma chemistry, ornithine
91 decarboxylase activity, polyamine concentrations, and the expression of various apoptotic

92 markers in fish during fresh water transfer. Finally, we studied the effects of polyamine
93 supplementation on active ion transport and membrane conductance in the opercular epithelium
94 under hypoosmotic conditions. The opercular epithelium has been used as a surrogate model of
95 the marine fish gill (Marshall, 2011; Marshall et al., 2000), and has been used to study the
96 mechanisms of cell volume regulation during osmotic challenges (Marshall et al., 2005). In this
97 study, we will assess the ability of polyamines to influence cell-swelling induced changes in
98 active ion transport in this epithelium.

99

100 **2. Materials and methods**

101

102 *2.1 Experimental animals*

103

104 Adult *F. grandis* were obtained from a local hatchery (Gulf Coast Minnows, Thibodeaux, LA)
105 and kept in the Life Sciences Aquatic Facility at Louisiana State University (Baton Rouge, LA,
106 USA). Fish were maintained in 5 ppt water for at least one month in a 570-liter glass aquarium
107 with mechanical and biological filtration, and UV-sterilization. Water salinity was monitored
108 using a water quality meter (YSI, Yellow Spring, OH, USA) and temperatures were maintained
109 at 22-24 °C. Fish were kept on a light cycle of 12 h light and 12 h dark provided by fluorescent
110 lighting set on an automatic timer. Fish were fed a commercial fish pellet (Cargill, Aquaxcell™
111 WW Fish Starter 4512, Franklin, LA, USA) twice daily at 2% body weight throughout
112 experimentation, and partial water changes were performed at least twice per week to keep water
113 quality constant.

114

115 *2.2 Experimental protocols*

116

117 *Series 1:* Blood plasma chemistry and gill surface morphology were assessed during acute
118 hypoosmotic challenges. One hundred and fifty adult fish (weight range 4.3-16.8 g) were
119 acclimated to 5 ppt water for at least one month. Immediately prior to sampling, a subset of fish
120 (n =6) were sampled as described below. The remaining fish were divided randomly into 5
121 groups, then transferred acutely to 5, 2, 1, 0.5, or 0.1 ppt water, which was made by diluting
122 Instant Ocean® salt (Blacksburg, VA, USA) with reverse osmosis water. At 6 h, 1 d, 3 d, or 7 d

123 post-transfer (n=6 per salinity per time point), fish were net-captured and anesthetized with 0.5
124 g/L tricaine methanesulfonate (MS-222). The tricaine stock solution (Finquel vet., Western
125 Chemicals Inc., Washington, USA) had a concentration of 4 mg/mL and was buffered to a pH
126 between 7 and 7.5 with Tris buffer (Trizma base, Sigma-Aldrich). Whole gill baskets were
127 dissected from fish and washed with Milli-Q-purified water for 10 s. The 3rd and 4th left gill
128 arches were fixed in a solution of 2% glutaraldehyde and 1% formaldehyde in 0.1 M cacodylate
129 buffer for scanning electron microscopic (SEM) analysis of the gill surface, as described in
130 Section 2.3. Blood was collected into micro-hematocrit capillary tubes (Fisher Scientific,
131 Pittsburgh, PA, USA) following caudal severance and centrifuged at 3,000 g for 3 min. Plasma
132 was collected and stored at -20 °C while awaiting analysis of plasma osmolality, as described in
133 Section 2.4.

134 *Series 2:* In these studies, the influence of inhibition of ornithine decarboxylase on plasma
135 osmolality, plasma Na⁺ and Cl⁻ concentrations, polyamine concentration and caspase-3 activity
136 were assessed during hypoosmotic exposure. Two hundred and forty adult *F. grandis* (weight
137 range 4.9-12.3 g) were acclimated to 5 ppt water, and fish were weighed and injected
138 intraperitoneally with 10 µL phosphate-buffered saline (PBS; sham control; 146 mM NaCl, 3
139 mM KCl, 15 mM NaH₂PO₄, 15 mM Na₂HPO₄, and 10 mM NaHCO₃ at pH 7.4) or DFMO (0.2
140 mg DFMO/µL PBS) per g fish for two days prior to hypoosmotic transfers. On day 3, half of the
141 fish in the DFMO and PBS treatments were transferred to 0.1 ppt water and the other half of the
142 remaining fish were transferred to 5 ppt water. Immediately prior to transfer, a subset of fish (n
143 =6) were sampled in both DFMO and PBS treatments. The remaining fish were injected daily
144 before morning feeding with either DFMO or PBS, as described above. PBS or DFMO was
145 injected intraperitoneally using a Hamilton microsyringe (Hamilton, Reno, NV, USA). Plasma
146 was collected from 120 fish using the same procedure, as described for Section 2.2 (Series 1),
147 and stored at -20 °C while awaiting analysis of plasma chemistry, as described in Section 2.4.
148 All four gill arches from these fish were flash frozen in liquid nitrogen and stored at -80 °C for
149 analysis of caspase-3 activity, as described in Section 2.6. Another 120 fish were net-captured
150 and anesthetized in 0.5 g/L tricaine methanesulfonate. Whole gill baskets were dissected from
151 fish and flash frozen in liquid nitrogen. The whole gill baskets were stored at -80 °C for analysis
152 of polyamine concentrations, as described in Section 2.7.

153 *Series 3:* The effects of salinity challenges on the mRNA levels of arginase II (*arg II*) and
154 ornithine decarboxylase (*odc*) in isolated mitochondrion-rich cells (MRCs) and pavement cells
155 (PVCs) of the gill epithelium were investigated. Forty-eight fish (weight range 8.19-17.83 g)
156 were acclimated in 5 ppt water for at least one month. Half the fish were transferred to 5 ppt
157 water and the other 24 fish were transferred to 0.1 ppt water. After 1 d post-transfer, fish were
158 net-captured and anesthetized in 0.5 g/L MS-222. Whole gill baskets were dissected from fish
159 and washed with ultrapure water for 10 s. MRCs and PVCs were isolated from pooled fish gills
160 (i.e., 2 gills per isolation) using the procedure described in (Galvez et al., 2002), with
161 modifications described below. Briefly, *F. grandis* fish gills were washed three-times in ice-cold
162 phosphate-buffered saline (137 mM NaCl, 4.3 mM Na₂HPO₄, 2.7 mM KCl, and 1.4 mM
163 NaH₂PO₄ at pH 7.8) for 10 min. Gill filaments were removed from their arches, cut into small
164 sections, and digested in 0.25% Trypsin-EDTA (Sigma, St. Louis, MO, USA) for 20 min at 300
165 RPM using a SK-300 shaker (Lab companion, Geumcheon-Gu, Seoul, Korea). Gill digests were
166 passed through a 96 µm mesh filter in 15 mL stop buffer (Kelly et al., 2000). Gills were trypsin-
167 digested 2 or 3 times to yield a mixed population of isolated gill cells, then centrifuged at 300 g
168 for 8 min at 4 °C. Gill cells were diluted in a 10-fold volume of PBS centrifuged at 500 g for 10
169 min at 4 °C. The pellet, which was resuspended in 2 mL PBS, was applied to the top of a
170 discontinuous Percoll gradient (Sigma, St. Louis, MO, USA) consisting of a 1.03 g/ml top layer,
171 a 1.06 g/ml middle layer, and a 1.09 g/ml bottom layer. The stacked cell suspension was
172 centrifuged (1,000 g for 35 min at 4 °C) to isolate PVCs and MRCs at the 1.03-1.06 g/mL and
173 1.06-1.09 g/mL Percoll interfaces, respectively. Each isolated cell fraction was stored at -80 °C
174 until RNA extraction, then analyzed by quantitative PCR for *arg II* and *odc* mRNA levels, as
175 described in Section 2.5.

176 *Series 4:* Killifish gill *c-fos* and *c-myc* mRNA transcript levels and caspase-3 activity were
177 assessed as putative measures of cell proliferation and cell apoptosis following acute freshwater
178 transfer. Sixty adult fish (weight range 3.83-12.61 g) were acclimated to 5 ppt water for at least
179 one month. Gills were sampled prior to transfer and at 6 h, 1 d, 3 d, and 7 d post-transfer to 5 ppt
180 or 0.1 ppt water (n=6 per salinity per time point). The first two left gill arches were immersed in
181 RNAlater and stored at 4 °C overnight, then transferred to -20 °C while awaiting total RNA
182 extraction and qPCR analyses of *c-fos* and *c-myc* transcript abundance, as described in Section

183 2.5. All four gill arches from the right side were flash frozen in liquid nitrogen, stored at -80 °C,
184 and used for analysis of caspase-3 activity, as described in Section 2.6.

185 *Series 5:* Tests were conducted to assess the putative role of polyamines in the compensatory
186 response of fish to hypoosmotic challenge. The opercular epithelium was used as a surrogate of
187 the fish gill to study the influence of polyamines on membrane conductance (G_t , mS cm^{-2}) and
188 short-circuit current (I_{sc} , $\mu\text{A cm}^{-2}$) (Marshall et al., 2000). Adult *F. grandis* were acclimated to 5
189 ppt water and anaesthetized in 0.2 g/L MS-222. Both opercular membranes of the fish were
190 isolated as described by Marshall et al (2000). Briefly, each operculum was mounted between
191 two plexiglass sliders (Physiological instruments, San Diego, CA, USA), exposing a 0.1 cm^2
192 diameter round aperture, and placed in individual Ussing chambers (Physiological Instruments,
193 San Diego, CA, USA) (Marshall et al., 2000). The Ussing chambers contained isotonic saline
194 (151 mM NaCl, 3 mM KCl, 0.88 mM MgSO_4 , 4.6 mM Na_2HPO_4 , 0.48 mM K_2HPO_4 , 1 mM
195 CaCl_2 , 11 mM HEPES-free salt, and 4.5 mM urea at an osmolality of 334 mOsm/kg and pH 7.8)
196 on each side of the membrane, as described previously (Daborn et al., 2001). The isotonic
197 bathing solution was bubbled with 100% oxygen. The basolateral side of the membrane was
198 bathed in 2 mL isotonic saline with 3 mM glucose added, whereas the apical side contained 2 mL
199 isotonic saline. I_{sc} and G_t across the opercular epithelium were measured in real time with a data
200 acquisition system (PowerLab and LabChart 7 software, ADInstrument Inc., CO, USA). A pulse
201 of 0.002 V was given every min to calculate G_t according to Ohm's law: $G_t = \Delta I_{sc} / \Delta V$. Once a
202 baseline was achieved under symmetrical conditions (isotonic saline on both sides of the
203 membrane), the isotonic solution was replaced with a hypotonic bathing solution (75% isotonic
204 saline, 25% distilled water) under symmetrical conditions, resulting in an osmolality of 270
205 mOsm/kg. This hypotonic solution mimicked the plasma osmolality of killifish during the early
206 stages of hypoosmotic shock, as described in Fig. 1.

207 I_{sc} and G_t were assessed in opercula immersed in isotonic (Iso) and hypotonic (Hypo) bathing
208 solutions for 30-45 min each to allow steady-state values to be reached. In order to derive the
209 relationship between changes in I_{sc} versus polyamine concentrations for each of the three
210 compounds, preliminary experiments were conducted. The results of preliminary experiments
211 showed that there was no significant difference in change of I_{sc} between low dose and high dose
212 of individual polyamines. A polyamine mixture consisting of 0.4 mM putrescine, 0.3 mM
213 spermidine, and 0.1 mM spermine was used in subsequent experiments as described below. First,

214 the influence of the polyamine mixture on the change of I_{sc} and G_t was assessed. Briefly, a
215 steady state of I_{sc} and G_t was attained under the Iso condition, then a polyamine mixture (0.4 mM
216 putrescine, 0.3 mM spermidine, and 0.1 mM spermine, PA) was added to the basolateral side of
217 opercular epithelia, either: a) coincident with transfer from isotonic to hypotonic conditions (pre-
218 PA, n =7), or b) following initial hypotonic transfer and establishment of a steady-state I_{sc} under
219 the hypotonic condition (post-PA, n =10). Second, the influence of individual polyamines on the
220 change in I_{sc} and G_t was assessed. Putrescine (PUT, 0.4 mM), spermidine (SPD, 0.3 mM), and
221 spermine (SP, 0.1 mM) were added individually to the basolateral side of the opercular
222 epithelium coincident with transfer from isotonic to hypotonic conditions (Hypo), respectively (n
223 =7 for Hypo + PUT, Hypo + SPD, and Hypo + SP). I_{sc} and G_t were recorded for 40 min until
224 reaching a steady-state and percent change of I_{sc} and G_t was calculated according to Equation 1,

$$225 \quad \text{Percent change} = \frac{\text{Value}_{\text{treat}} - \text{Value}_{\text{isotonic}}}{\text{Value}_{\text{isotonic}}} \times 100\% \quad (1)$$

226 where $\text{Value}_{\text{treat}}$ represents the values of I_{sc} or G_t at pre-PA and post-PA in Iso conditions, Hypo
227 alone, Hypo + PUT, Hypo + SPD and Hypo + SP at different time points. $\text{Value}_{\text{isotonic}}$ indicates
228 a steady-state of I_{sc} or G_t when opercular epithelia were incubated in isotonic saline.

229

230 2.3 Scanning electron microscopy (SEM) analyses

231

232 Gills were fixed in 2% glutaraldehyde and 1% formaldehyde in 0.1 M cacodylate buffer (pH
233 7.4-7.6) for 4 h, rinsed in 0.1 M cacodylate buffer containing 0.02 M glycine, post-fixed in 2%
234 osmium tetroxide for 1 h, and rinsed in water. Samples were dehydrated in an ethanol series (10
235 min at 50%, 10 min at 70%, 10 min at 80%, 2 rinses of 10 min at 95%, and 3 rinses of 15 min at
236 100% ethanol), dried with liquid CO_2 in a Denton critical point dryer (Cherry Hill, NJ, USA)
237 mounted on aluminum SEM stubs and coated with a gold:palladium solution (V:V of 60:40) in
238 an Edwards S150 sputter coater (Ashbord, Kent, UK). The afferent edge of each gill filament
239 was randomly imaged using a JSM-6610 high vacuum mode SEM (Tokyo, Japan).

240

241 2.4 Plasma chemistry analyses

242 Plasma osmolality was analyzed by freeze-point depression (Precision systems INC, Natick,
243 MA, USA). Plasma Na⁺ concentrations were measured using flame atomic absorption
244 spectroscopy (Varian Australia Pty Ltd, Australia), and plasma Cl⁻ concentrations were measured
245 using a modified mercuric thiocyanate method (Zall et al., 1956).

246

247 *2.5 Relative arg II, odc, c-myc, and c-fos mRNA levels*

248

249 Commercial SYBR Green master mix (QIAGEN Inc. Valencia, CA, USA) was used to
250 analyze the relative mRNA levels of *arg II*, *odc*, *c-myc*, *c-fos*, and the reference gene, 18S
251 ribosomal RNA (*18s rRNA*). Expressed sequence tags (ESTs) for *arg II* (GenBank accession no.
252 AB290198.1), *odc* (GenBank accession no. CN977303.1), *c-fos* (GenBank accession no.
253 DN956552.1) and *c-myc* (GenBank accession no. CN985702.1) from *F. heteroclitus* were
254 obtained from the National Center for Biotechnology Information database
255 (<http://www.ncbi.nlm.nih.gov/>). Primers for quantitative PCR were developed for all genes
256 using Integrated DNA Technologies Inc. software (Coralville, IA, USA) (Table 1). A 20 µL
257 reaction mixture (0.1 µg cDNA, 10 nM forward and reverse primers, 5 µL SYBR Green reagents)
258 was used for the ABI Prism 7000 SDS system (Carlsbad, CA, USA). The first strand of cDNA
259 was reverse-transcribed from total mRNA of MRCs and PVCs isolated from the fish gill.
260 Samples were cycled 40 times at 95 °C for 15 s and 60 °C for 1 min. Efficiency and relative
261 changes in mRNA levels were calculated using the 2^{-ΔΔCt} method (Fleige et al., 2006).

262

263 *2.6 Caspase-3 activity assay*

264

265 A caspase-3 assay kit (Sigma, St. Louis, MO, USA) was employed to measure caspase-3
266 activity, which is based on the hydrolysis of acetyl Asp-Glu-Val-Asp 7-amido-4-methylcoumarin
267 by caspase 3 that results in the release of the fluorescent 7-amino-4-methylcoumarin. Gill arches
268 were homogenized with a 10-fold volume of 0.85% NaCl, and the original homogenate was used
269 directly to measure caspase-3 activity. Gill homogenates were diluted 20-fold and measured for
270 total protein (Sigma, St. Louis, MO, USA). Fluorescence intensity was measured with excitation
271 at 355 nm and emission at 460 nm using a VICTORTM X3 multilabel plate reader (Perkin Elmer,
272 Santa Clara, CA, USA). A 1x assay buffer of 200 µl served as a blank to adjust the fluorimeter

273 to zero. Fold-change in gill caspase-3 activity was calculated by taking the ratio of the
274 enzymatic activity of post-transfer to 5 ppt water and 0.1 ppt water over the enzymatic activity of
275 pre-transfer at each time point.

276

277 *2.7 Gill polyamine contents*

278

279 Gill baskets were thawed and homogenized with methanol (containing 0.1 mM HCl) (V:V
280 for 1:3) in dry ice using a PRO200 Homogenizer (Lab depot Inc. Dawsonville, GA, USA).
281 Samples were incubated in 0.6 M perchloric acid to extract polyamines and derivatized with o-
282 toluoyl chloride using a slightly modified procedure from that described previously (Wongyai et
283 al., 1988). Samples (20 μ L) were then analyzed for polyamines by high performance liquid
284 chromatography (HPLC) (Bio-Rad high-performance liquid chromatograph gradient module
285 with a Model 996 photodiode array detector; Milford, MS, USA). HPLC separations were
286 performed using an ACE C-18-PFP column (150 mm x 4.6 mm; 5 μ m; Chadds Ford, PA, USA),
287 a mobile phase consisting of 0.1% trifluoroacetic acid in water and 0.1% trifluoroacetic acid in
288 acetonitrile, with a flow rate of 1.0 mL/min, and UV detection at 254 nm. Each polyamine
289 derivative was dissolved separately in water to yield stock solutions of 200 nmol /100 μ L. A
290 series of standard solution containing 53 to 1500, 144 to 2300, and 25 to 400 ng/100 μ L of
291 putrescine, spermidine and spermine, respectively, were prepared by serial dilution of the stock
292 solutions with water. Each sample including standards was analyzed in triplicate, and an average
293 peak area under the curve was obtained for each sample.

294

295 *2.8 Statistical analysis*

296

297 Results were presented as mean \pm standard error of the mean (SEM). Statistical differences
298 in plasma osmolality, mRNA transcript abundance, and I_{sc} and G_t between treatments were
299 analyzed using a one-way ANOVA (v.9.3, SAS Institute Inc., Cary, NC, USA) followed by a
300 LSD post hoc test. Statistical differences were considered significant at a P -value of 0.05 or less.

301

302 **3. Results**

303

304 3.1 Plasma chemistry

305

306 Initial experiments were performed to assess the influence of comparably small changes in
307 environmental salinity on plasma osmolality (Fig. 1) and gill surface morphology (Fig. 2). The
308 magnitude of the reduction of plasma osmolality disturbances depended on the severity of the
309 hypoosmotic transfer and on the time following post-transfer. Plasma osmolality decreased by
310 approximately 19.5% following transfer from 5 ppt water to either 0.1 ppt or 0.5 ppt water,
311 reaching their lowest values at 1 d and 6 h, respectively (Fig. 1). Plasma osmolality in the 0.5
312 ppt treatment recovered to its original level by 1 d, but it did not completely recover to the pre-
313 transfer value even after 7 d in the 0.1 ppt treatment ($P=0.007$). In comparison, plasma
314 osmolality in *F. grandis* was not affected by the abrupt transfer from 5 ppt to 1 ppt, 2 ppt, or 5
315 ppt water at any time during the 7 d post-transfer period.

316

317 3.2 Gill morphology

318

319 Scanning electron microscopy was used to assess the morphology of the apical opening of
320 MRCs on the gill surface of fish undergoing osmotic shock, as described in Section 2.3. The gill
321 surface of fish acclimated to salinities of 1 to 5 ppt water consisted of pavement cells (PVCs)
322 possessing concentric rings of microridges around the outer cell margins, and, on occasion,
323 microvilli projecting towards the center of cells (Fig. 2). MRCs in fish gills exposed to 5 and 2
324 ppt water were predominately SW-type, as noted by their small apical openings at the gill surface
325 localized at the afferent edge of the filamental epithelium. Exposure to 1 ppt water led to minor
326 changes in the surface appearance of the fish gill, with a slight enlargement of MRCs during the
327 initial 6 h to 1 d post-transfer. FW-type MRCs, characterized by their convex shape and well-
328 developed microvilli, began to emerge on the gill surface as salinity decreased to 0.5 ppt and
329 below. These cell types were only expressed transiently, being replaced by SW-type MRCs,
330 which reemerged by 3 d at 0.5 ppt or by 7 d at 0.1 ppt. Regardless, FW-type MRCs with smaller
331 apical openings were still present following 7 d exposure to 0.1 ppt and 0.5 ppt water (Fig. 2).

332

333 3.3 *argII* and *odc* mRNA levels in pavement cells and mitochondrion-rich cells

334

335 The mRNA levels of *argII* and *odc* in MRCs and PVCs isolated from the gills of 5 ppt and
336 0.1 ppt fish were assessed. Compared to the PVCs at 5 ppt, the levels of *arg II* and *odc* mRNA
337 in MRCs did not change. During hypoosmotic exposure, *arg II* (Fig. 3 A) and *odc* (Fig. 3B)
338 mRNA levels were 4.5-fold ($P=0.022$) and 2.6-fold ($P=0.011$) higher in MRCs relative to PVCs,
339 respectively. In contrast, *arg II* and *odc* mRNA levels increased by 3.3-fold ($P=0.005$) and 5.8-
340 fold ($P=0.001$) in MRCs after 0.1 ppt water compared to the 5 ppt control (Fig. 3).

341

342 3.4 Plasma chemistry during *Odc* inhibition

343

344 Administration of DFMO inhibited gill ODC activity and polyamine levels, and also reduced
345 the magnitude of the plasma osmotic (Fig. 4A), hyponatremic (Fig. 4B), and hypochloremic (Fig.
346 4C) responses measured in fish following transfer to 0.1 ppt water. Transfer to 0.1 ppt water
347 reduced plasma osmolality in both the sham and DFMO-treated fish, although the reduction was
348 more pronounced in the sham treated fish ($P=0.029$). Plasma Na^+ concentrations were reduced
349 by 14% at 6 h and 18% at 1 d in sham fish transferred to 0.1 ppt water compared to the pre-
350 transfer levels of sham fish at 5 ppt. In fish administered DFMO, plasma Na^+ was reduced only
351 by 7.7% ($P=0.046$) and 15.4% ($P=0.021$) at 6 h and 1 d post transfer to 0.1 ppt, respectively (Fig.
352 4B). Similarly, the magnitude of the hypochloremic effect of 0.1 ppt transfer was attenuated by
353 DFMO administration compared to that seen in the sham controls at 6 h ($P=0.013$) and 1 d
354 ($P=0.016$) transfer to 0.1 ppt (Fig. 4C). Both plasma Na^+ and Cl^- returned to pre-transfer levels
355 after 3 d of hypoosmotic exposure in sham controls and the DFMO-treated fish. In comparison
356 to the differences seen in the 0.1 ppt exposed fish, plasma osmolality, plasma Na^+ , and plasma
357 Cl^- were not significantly different between the DFMO-treated fish and PBS-treated fish
358 maintained in 5 ppt water over time (Fig. 4). These data suggest that the reduction in the
359 hypoosmotic effects of 0.1 ppt water by administration of DFMO was not simply due to the drug
360 serving as an osmolyte.

361

362 3.5 Polyamine concentration with or without *Odc* inhibition

363 The sum total of putrescine, spermidine and spermine concentrations were measured in the
364 gills of fish acclimated to 5 ppt and 0.1 ppt with and without the concomitant inhibition of *Odc*

365 activity with DFMO. When fish were acclimated to 5 ppt water, the polyamine levels in the PBS
366 injection group (sham control) did not vary over time, whereas they increased by 23.8%, 62.8%,
367 46.8%, and 30.0% at 6 h, 1 d, 3 d, and 7 d, respectively, when transferred to 0.1 ppt. When fish
368 were kept in 5 ppt water, inhibition of Odc activity using DFMO decreased the sum of
369 polyamine concentrations by 31.5%, 39.7%, 38.4% and 72.5% comparing to the sham control at
370 6 h, 1 d, 3 d, and 7 d, respectively. In comparison, when Odc activity was inhibited in fish
371 transferred to 0.1 ppt water, the gill polyamines concentrations decreased by 32.5%, 49.2%, 54.8%
372 and 64.0% comparing to the sham control at 6 h, 1 d, 3 d, and 7 d, respectively (Table 2).

373

374 3.6 Relative *c-myc* and *c-fos* mRNA levels and caspase-3 activity in gill

375

376 The mRNA levels for *c-fos* and *c-myc* were measured in the gills following hypoosmotic
377 exposure as a measure of cell proliferation in the tissue. Gill *c-fos* mRNA expression increased
378 14.1-fold at 6 h ($P=0.001$) and 3.5-fold at 1 d ($P=0.027$) following transfer to 0.1 ppt water
379 (compared to the pre-transfer control levels), but returned to the pre-transfer level by 3 d (Fig.
380 5A). Compared to the 5 ppt control, the *c-fos* mRNA level increased 10.5-fold and 4.4-fold at 6
381 h and 1 d, respectively, following hypoosmotic exposure ($P<0.020$ for both time points) (Fig.
382 5A). Gill *c-myc* mRNA abundance was increased 6.1-fold after 6 h of hypoosmotic exposure,
383 but returned to the pre-transfer level at 7 d (Fig. 5B). The level of *c-myc* mRNA increased up to
384 7.1-fold by 1 d post-transfer (compared to the pre-transfer level) ($P<0.001$) (Fig. 5B). The
385 mRNA expression of *c-myc* increased at 6 h, 1 d, and 3 d in the gills of 0.1 ppt-acclimated fish
386 ($P=0.018$, 0.025 and 0.011, respectively) compared to the 5 ppt control at the same time points
387 (Fig. 5B).

388 The onset of apoptosis was assessed by analyzing caspase-3 activity in gill. In an initial
389 experiment, gill caspase-3 activity increased approximately 3-fold following 3 d of hypoosmotic
390 exposure ($P=0.006$) but returned to the control level at 7 d (Fig. 5C). In comparison, caspase-3
391 activity in the gill did not change significantly during exposure to 5 ppt water over 7 days (Fig.
392 5C). In a second experiment, caspase-3 activity and the influence of Odc inhibition with DFMO
393 on caspase-3 activity during concomitant hypoosmotic challenge were assessed. Inhibition of
394 Odc activity using DFMO was found to have no effect on gill caspase-3 activity in fish
395 maintained at 5 ppt compared to the 5 ppt sham controls. The 0.1 ppt sham control continued to

396 show a significant increase in caspase-3 activity at 6 h and 1 d ($P<0.001$ for both time points)
397 before returning to the control level (Fig. 5D). In comparison, inhibition of Odc activity with
398 DFMO decreased the ability of the hypoosmotic treatment to induce gill caspase-3 activity. In
399 the 0.1 ppt DFMO treatment, gill caspase-3 activity was not increased above the level of the 5
400 ppt sham control (Fig. 5D).

401

402 *3.7 The effect of polyamines on opercular I_{sc} and G_t*

403

404 The influence of a polyamine mixture (0.4 mM putrescine, 0.3 mM spermidine, and 0.1 mM
405 spermine, PA) on the hypotonic-induced changes in I_{sc} and G_t in the opercular epithelium was
406 investigated. After transfer to the hypotonic solution, I_{sc} of the opercular epithelium decreased
407 immediately, and reached a new steady state within 30-35 min (Fig. 6A). Hypotonic shock
408 induced a 52% reduction in I_{sc} compared to that measured in the isotonic medium (Fig. 6A).
409 Compared to the hypotonic control, pre-PA significantly inhibited I_{sc} reduction in the opercular
410 epithelium after 20 min hypotonic exposure, reaching its maximum inhibition at 40 min
411 ($P=0.001$) (Fig. 6A). However, post-PA did not affect I_{sc} compared to the hypotonic control
412 over time (Fig. 6A). Transfer of the opercular epithelium to the hypotonic solution immediately
413 reduced its G_t and it remained at this level for at least 40 min (Fig. 6B). Application of PA either
414 before hypotonic transfer (pre-PA) or after immediately after hypotonic transfer (post-PA) did
415 not significantly affect this hypotonically-induced inhibition of G_t (Fig. 6B). Additional
416 experiments were conducted to assess the contribution of individual polyamines to changes in I_{sc}
417 and G_t during hypotonic shock. The I_{sc} and G_t of the opercular epithelium were decreased
418 immediately after transfer to the hypotonic solution, reaching new steady states within 30-35 min
419 (Fig. 7A). When individual polyamines were applied, only spermidine was shown to attenuate
420 the hypotonically-induced reduction in I_{sc} and G_t over time (Fig. 7B). In comparison, application
421 of putrescine or spermine did not affect the ability of hypotonicity to reduce the I_{sc} and G_t of the
422 opercular epithelium over time (Fig. 7B).

423

424 **4. DISCUSSION**

425

426 *4.1 Plasma chemistry and gill epithelial morphology*

427

428 In the present study, *F. grandis* were acutely transferred to salinities ranging from 5 ppt to
429 0.1 ppt water following acclimation to 5 ppt water (~15 % sea water). Salinities at or above 1
430 ppt did not impair plasma osmotic balance nor produce any notable morphological alterations to
431 the gill. In comparison, plasma osmolality was significantly reduced at 6 h post-transfer to 0.5
432 ppt water but recovered back to the 5 ppt control level within 1 d (Fig. 1). When fish were
433 transferred to 0.1 ppt water, plasma osmolality was reduced to the same extent as measured in
434 the 0.5 ppt treatment, although osmotic balance did not return to pre-transfer levels even after 14
435 days of exposure (Fig. 1). Water at 1 ppt water has 14 mM Na⁺, which is about 11-fold lower
436 than the extracellular fluid, whereas 0.5 ppt water has 7 mM Na⁺, which is approximately 22-fold
437 lower than that measured in the extracellular fluid. This represents a two-fold difference in the
438 ionic gradient between the blood and the outside environment despite only a 0.5 ppt difference in
439 salinity (0.5 ppt versus 1 ppt). One could also conclude that an approximate 20-fold dilution of
440 the environment compared to the blood is enough to differentiate between a physiological benign
441 and a physiological stressful salinity. Furthermore, the change in osmolality (about 73
442 mOsm/Kg) was larger than the sum of Na⁺ and Cl⁻ changes (25 and 30 mM), suggesting that the
443 regulation of other plasma ions was adversely affected at these low salinities. Osmotic
444 imbalance in dilute environments (0.5 ppt and below) may also be explained by the reduction in
445 the concentration of other ions in salt water such as calcium. For instance, a 22-fold dilution of
446 reconstituted sea water would lower the Ca²⁺ concentration to approximately 500 μM, which
447 represents a concentration only slightly higher than the Michaelis-Menten constant for the high
448 affinity Ca²⁺ transport in freshwater-acclimated *F. heteroclitus* (Patrick et al., 1997).

449 The multifunctionality of MRCs with environmental salinity has been demonstrated
450 (Marshall and Bryson, 1998), and shown in euryhaline *Fundulus* species to transition from a
451 seawater to a freshwater phenotype within a narrow range of salinity well below the isosmotic
452 point of the extracellular fluid (Copeland, 1950; Whitehead et al., 2011b; Whitehead et al., 2012).
453 In the current study, gill MRC cell types were identified using SEM (Goss et al., 1994; Perry et
454 al., 1992). The apical surface of the gill MRCs of *F. grandis* retained an apical crypt
455 characteristic of a seawater fish gill at a salinity of 1 ppt and above. Only when acutely exposed
456 to a salinity at or below 0.5 ppt did the apical surface of MRCs in the fish gill attain a concave
457 appearance more characteristic of a freshwater gill phenotype (Fig. 2). Although the

458 functionality of these putative MRC subtypes is not known, this phenotypic transition only
459 occurred in treatments that also led to an impairment in plasma osmolality regulation (Fig. 1). At
460 salinity challenges at which plasma osmolality was reduced, there was a tendency towards
461 expression of MRCs on the gill surface that were of freshwater phenotype (Fig. 2). It has been
462 demonstrated that MRCs alternate their morphology in response to abrupt environmental osmotic
463 change (Copeland, 1950; Kaneko and Katoh, 2004; Katoh et al., 2001; Katoh et al., 2000;
464 Laurent et al., 2006). Fish exposed to salinities of 0.1 ppt and 0.5 ppt exhibited few SW-type
465 MRCs in their gills after 6 h. These cells were replaced by large MRCs that were predominantly
466 triangular in shape and with apical surfaces that contained short microvilli flush with the
467 surrounding PVCs (Fig. 2). The actual fate of these seawater MRCs during hypoosmotic transfer
468 is unclear. Laurent and others (Laurent et al., 2006) suggested that seawater MRCs either
469 undergo apoptosis, necrosis, exfoliation, or are simply covered by pavement cells, where they
470 remain dormant in the underlying tissue during bouts of fresh water exposure. These FW-type
471 MRCs were termed cuboidal cells, and were characterized by their wedge-like appearance
472 between neighboring PVCs, analogous to the mitochondrion-rich PVCs described in rainbow
473 trout (Galvez et al., 2002; Laurent et al., 2006). With continued extreme hypoosmotic exposure,
474 the surface exposure of these cuboidal cells decreased over time and SW-type apical crypts
475 emerged, even in fish acclimated to 0.1 ppt water (Fig. 2). This produced a mixed population of
476 SW and FW MRCs, as previously described (Laurent et al., 2006; Scott et al., 2008; Scott et al.,
477 2006; Whitehead et al., 2012). This ability to rapidly cover and uncover cell types is beneficial
478 for euryhaline fish species such as *F. grandis*, which may need to under quick physiological
479 transitions during fluctuations in environmental salinity but probably do so at a high energetic
480 cost (Kidder et al., 2006). It is unclear why SW MRCs began to resurface in the 0.1 ppt- and 0.5
481 ppt-acclimated fish gill, although this capacity benefits *F. grandis* survival in unstable
482 environments. Alternatively, the need for MRCs in dilute environments (i.e., 0.5 ppt and below)
483 may relate to the active calcium uptake that occurs in parallel with monovalent ion transport in
484 FW (and SW) ionocytes (Evans et al., 2005; Marshall and Bryson, 1998). Regardless, these data
485 support a dynamic restructuring of the gill epithelium of *F. grandis* at low environmental salinity.

486 In individual multifunctional MRCs, many transport systems including ion pumps,
487 cotransporters, channels and exchangers operate simultaneously to facilitate active ion secretion
488 in marine water or active ion absorption in fresh water (Hiroi and McCormick, 2012; Marshall

489 and Grosell, 2005). The current model of active ion secretion in the marine fish gill involves a
490 basolateral Na^+, K^+ -ATPase, which provides the driving force for Na^+ and Cl^- entry via a
491 $\text{Na}^+, \text{K}^+, 2\text{Cl}^-$ cotransporter (NKCC), and the accumulation of Cl^- to facilitate its passive
492 movement across the apical membrane into the water via the anion channel Cystic Fibrosis
493 Transmembrane conductance Regulator (CFTR) (Marshall et al., 1999). Reduction of plasma
494 osmolality during exposure to low environmental salinity causes immediate MRC swelling and
495 inhibit active Cl^- secretion (Marshall, 2011). With prolonged exposure to fresh water,
496 morphological alterations to the gill would include the expression of MRC types that participate
497 in active ion absorption rather than in active ion secretion. Although the exact model of active
498 Na^+ transport varies between species, *Fundulus* lack an active Cl^- absorption mechanism in the
499 gill (Scott et al., 2004). As such, the regulation of paracellular Cl^- loss is particularly relevant in
500 killifish. The ability to mitigate the diffusive loss of Cl^- upon acute transfer to fresh water is a
501 feature defining freshwater-tolerant killifish species or populations of euryhaline species best
502 adapted to tolerate hypoosmotic exposure (Brennan et al., 2015; Scott et al., 2004; Scott and
503 Schulte, 2005; Scott et al., 2006; Whitehead et al., 2011a; Whitehead et al., 2011b; Whitehead et
504 al., 2012). The appearance of cuboidal cells presumably would help to inhibit ion loss at the gill
505 epithelium and maintain plasma ion concentrations in response to rapid fluctuations in
506 environmental salinity.

507

508 *4.2 Possible roles of polyamines in cell apoptosis and cell proliferation*

509

510 In the present study, *arg II* and *odc* mRNA levels were significantly higher in MRCs than in
511 PVCs regardless of salinity, and the concentrations of both transcripts were further increased in
512 freshwater-type MRCs following transfer to 0.1 ppt water (Fig. 3). Arginase II is abundant in
513 extrahepatic cells rich in mitochondria, where it may be involved in numerous physiological
514 functions including glutamate, proline, and polyamine biosynthesis, or in the modulation of nitric
515 oxide synthesis (Morris, 2004). The concurrence of elevated *arg II* and *Odc* mRNA levels in gill
516 MRCs (Fig. 3) and gill MRC remodeling (Fig. 2) suggests that polyamines may be associated
517 with the phenotypic plasticity of MRCs in the fish gill (Brennan et al., 2015; Whitehead et al.,
518 2011b; Whitehead et al., 2012). A similar relationship between hypoosmotic challenge and *Odc*
519 activity was described in the gills of *F. heteroclitus* (Whitehead et al., 2012) and brine shrimp

520 (Watts et al., 1996) and in the variant L1210 mouse leukemia cell line (Uthaiwan et al., 2001).
521 As a key enzyme for polyamine biosynthesis, Odc upregulation suggests a link between
522 polyamine biosynthesis and hypoosmotic exposure.

523 Polyamines have an important role in RNA transcription, cell growth, cell proliferation, and
524 apoptosis (Pegg and McCann, 1982; Ray et al., 1999; Tabor and Tabor, 1984). Previous studies
525 have shown that polyamines can positively regulate *c-fos*, *c-ras*, and *c-myc* transcription, and that
526 inhibition of Odc activity using DFMO can inhibit *c-myc* and *c-fos* mRNA expression in
527 carcinoma cells in primary cultured rat kidney cells (Tabib and Bachrach, 1994). Evidence is
528 provided here that ornithine decarboxylase, or putrescine and other polyamines produced
529 irreversibly by Odc, may influence the compensatory response to hypoosmotic acclimation in
530 fish. An increase in caspase-3 activity to environmental stress including osmotic challenges has
531 been previously documented in fish (Krumnschnabel and Podrabsky, 2009). An increase in
532 caspase-3 activity has been shown in zebrafish (*Danio rerio*) during DNA damage (Lee et al.,
533 2008), in Atlantic salmon (*Salmo salar*) during hyperthermia (Takle et al., 2006), in sea bass
534 (*Dicentrarchus labrax L.*) during bacterial infection (Reis et al., 2007), in rainbow trout
535 (*Oncorhynchus mykiss*) after hyperosmotic transfer (Rojo and Gonzalez, 1999), and in sturgeon
536 (*Acipenser schrenckii*) during prolonged hypoxia (Lu et al., 2005). The role of caspase-3 in fish
537 correlates with extensive apoptosis and morphological abnormalities in tissues (Yamashita et al.,
538 2008). Inhibition of Odc activity with DFMO inhibited the ability of hypoosmotic exposure to
539 stimulate caspase-3 activity in the gill (Fig. 5). These results are consistent with the inhibitory
540 effects of DFMO on caspase-3 activity in intestine (Deng et al., 2005; Ray et al., 2000), bone
541 marrow stromal cells (Muscarì et al., 2005) and in cardiac myoblasts (Tantini et al., 2006).
542 DFMO also reduced gill polyamine concentrations in fish acclimated to 5 ppt and in fish
543 transferred acutely from 5 ppt to 0.1 ppt water. These data suggest that Odc activity is critical
544 for the continual production of endogenous polyamines in the fish gill and that these polyamines
545 can be reduced in concentration when Odc activity is inhibited. Furthermore, inhibition of Odc
546 significantly affected the capacity of fish gills to stimulate polyamine synthesis during a
547 hypoosmotic challenge.

548 Although the role of polyamines in gill remodeling remains unclear, marine *Fundulus* species
549 that are not able to physiological transform their gills to a freshwater phenotype nor able to
550 survive hypoosmotic transfer following acclimation to sea water, have a reduced capacity to

551 stimulate polyamine biosynthetic pathways compared to euryhaline, *F. heteroclitus* (Brennan et
552 al., 2015). The fact that the increase in polyamine levels occurred concomitantly with an
553 increase in gill caspase-3 activity following 0.1 ppt water exposure (Fig. 5C) demonstrated that
554 polyamines may induce apoptosis in gills mediated through a caspase pathway. Although the link
555 between polyamines and phenotypic plasticity to environmental stress such as that induced by a
556 hypoosmotic challenge is unclear, several possible mechanisms are worth considering. First,
557 polyamines may induce cell apoptosis by triggering the c-Myc or c-Fos pathway in gills (Fig. 5A
558 and 5B). Increasing polyamine levels after 6 h and 1 d following FW-exposure (Table 2) were
559 concomitant with an increase in *c-myc* and *c-fos* mRNA levels in killifish gills (Fig. 5A, 5B).
560 The correlation between polyamine levels and the *c-myc* and *c-fos* mRNA levels was described
561 in a previous study in rat kidney cells (Tabib and Bachrach, 1994). These studies suggest that
562 polyamines have the ability to increase *c-fos* and *c-myc* mRNAs levels during environmental
563 challenges. The relationship between the increase in polyamine levels and the increase in *c-fos*
564 and *c-myc* mRNA levels during the first few days following hypoosmotic transfer (Fig. 5A, 5B)
565 support a causal relationship between these variables. Second, polyamines may trigger the
566 intrinsic cell apoptosis via the caspase pathway in the gills (Fig. 5C and 5D). The transient
567 increase in gill polyamine levels and the simultaneous increase in the mRNA levels of pro-
568 apoptotic factors and in the activity of markers of apoptosis, are intriguing and worth future
569 study.

570

571 *4.3 The influence of polyamines on the electrophysiological properties of the opercular* 572 *epithelium*

573

574 Besides cell apoptosis and proliferation, polyamines have been implicated in the regulation
575 of cell volume during hypotonic challenges (Watts et al., 1996). In order to test this hypothesis,
576 the opercular epithelium of killifish was used as a surrogate epithelium to the fish gill due to its
577 high abundance of MRCs, the presence of active Cl⁻ secretion similar to that found in the marine
578 fish gill, the existence of an electrical current under symmetrical conditions associated almost
579 entirely with this active Cl⁻ secretion, and the fact that this electrical current is almost entirely
580 inhibited by exposure to hypotonic media due to epithelial cell swelling (Marshall, 2011;
581 Marshall et al., 2000; Marshall et al., 2005). In this tissue, I_{sc} in the opercular epithelium of

582 brackish and marine acclimated killifish is almost entirely due to Cl^- secretion via the combined
583 actions of NKCC and CFTR (Karnaky et al., 1977).

584 The goal was to assess the influence of polyamines on the Cl^- -mediated short circuit current
585 (I_{sc}) before and after hypotonic exposure. The hypothesis was that polyamines would enhance the
586 ability of hypotonic exposure to reduce I_{sc} , which in a whole animal would attenuate the
587 diffusive loss of Cl^- and presumably enhance freshwater tolerance. As observed in previous
588 studies (Marshall et al., 2000), the I_{sc} of opercular epithelium (i.e., NaCl secretion) was reduced
589 by approximately 60%-70% within minutes of transfer from isotonic to hypotonic conditions
590 (Fig. 6). Despite the expectation that polyamines would actually stimulate a further reduction in
591 I_{sc} with hypotonic exposure, polyamines inhibited the hypotonically-induced attenuation of I_{sc}
592 (Fig. 7A) and G_t (Fig. 7 B). Surprisingly, these data suggest that polyamines function to inhibit
593 the ability of the MRCs in fish epithelia to reduce active Cl^- secretion during hypotonic exposure.
594 Additional experiments suggested that this effect of polyamines was mediated almost exclusively
595 by micromolar concentrations of extracellular spermidine. These data suggest that polyamines
596 function to inhibit the ability of the MRCs in fish epithelia to reduce active Cl^- secretion during
597 hypotonic exposure. This seemingly paradoxical response on isolated opercular epithelia was
598 independently validated in whole animal experiments in which endogenous polyamine
599 production during hypoosmotic exposure was blocked by administration of DFMO. It was found
600 that when polyamine concentrations were significantly reduced, even following freshwater
601 transfer, there was actually less of a reduction in the osmolality, and Na^+ and Cl^- concentrations
602 of plasma of fish transferred to 0.1 ppt water. In other words, polyamines enhanced rather than
603 reduced the osmolyte imbalance during hypoosmotic shock.

604 Many different mechanisms could probably function to reduce the hypotonic response in the
605 opercular epithelium. Polyaminated polyamines such as spermine are strong agonists of the
606 calcium-sensing receptor (CaSR) and produce a transient peak and sustained rise in intracellular
607 Ca^{2+} (Quinn et al., 1997). Previous studies have shown that the CaSR can regulate fluid
608 secretion in rat colonic crypts by increasing intracellular D-myo-inositol 1,4,5-trisphosphate
609 (IP3), which stimulates an increase in intracellular Ca^{2+} (Cheng et al., 2004). Extracellular
610 spermine and external Ca^{2+} appear to modulate the sensitivity of the colonic epithelial CaSR to
611 Ca^{2+} stimulated NKCC and CFTR mediated Cl^- secretion. CaSR is expressed in gill and other
612 fish epithelia, where it is thought to participate in systemic calcium homeostasis and

613 intracellular ion sensing (Loretz, 2008), and recently as a mechanism for protecting against Ca^{2+} -
614 induced cytotoxicity (Gu et al., 2014). In killifish, the hypotonic response in the gills and
615 opercular epithelium results in an increase in intracellular Ca^{2+} mediated through an alpha-2
616 adrenergic pathway independent of adenylyl cyclase (e.g. (Marshall et al., 1993)). However,
617 unlike in mammalian systems, this hypotonically-induced rise in intracellular Ca^{2+} inhibits rather
618 than increases NaCl secretion. Although a link between polyamines, CaSR, intracellular Ca^{2+} ,
619 and suppression of active ion secretion in the gills and opercular epithelium of fish during
620 hypotonic stress is not known, it is possible that polyamines prolong the survival of SW type
621 ionocytes in very dilute environments. DMFO may reduce the immediate effects of polyamines,
622 thus blunting hypotonic inhibition of NaCl secretion and may lead to early apoptosis of seawater
623 ionocytes and their replacement by FW-type ionocytes. It would be worth considering whether
624 polyamines interfere with Ca^{2+} responses either by blocking some downstream response of
625 intracellular signaling or by reducing the rise in intracellular Ca^{2+} during hypotonic shock.

626 In the long term, induction of polyamine synthesis during hypotonic exposure may facilitate
627 apoptosis of SW type MRCs and result in their replacement by FW type MRCs. Polyamines may
628 stimulate cell apoptosis and cell proliferation with the goal of remodeling the gill, especially in
629 MRCs. However, in the short term, polyamines appear to inhibit the ability of hypotonic cell
630 swelling to attenuate NaCl secretion in the operculum. Further studies are needed to determine
631 the role of polyamines in cell volume regulation, gill remodeling, or in osmotic sensing.

632 **Table 1**633 Sequences of forward and reverse primers used for amplification of *F. grandis*, *c-myc*, *c-fos*, *arg*634 *II*, *odc*, and *18s rRNA* amplicons for quantitative RT-PCR analysis.

635

Name	Direction	Sequence 5' → 3'
<i>c-myc</i>	Forward	TGCTTGTGCCTCTCACCAGTTCTA
<i>c-myc</i>	Reverse	AGCCTTCGAATCCTCCACGTTCTT
<i>c-fos</i>	Forward	ATCTGACAGCATCAAGTGCCTCCT
<i>c-fos</i>	Reverse	AGGTCTGGACGTTGCAGACTTCAT
<i>argII</i>	Forward	CAGCTGTGGTTACTGCATTGCGTT
<i>argII</i>	Reverse	ACAGGAAGCAACAAACCAGCACAG
<i>odc</i>	Forward	TTGCCACGCCAATGTGGTCTAA
<i>odc</i>	Reverse	ATGCTCCTGTCAAGTAACTGGCCT
<i>18s rRNA</i>	Forward	TTCCGATAACGAACGAGAC
<i>18s rRNA</i>	Reverse	GACATCTAAGGGCATCACAG

636

637 Table 2 The total gill polyamine concentrations, which represent the sum concentrations of gill
 638 putrescine, spermidine, and spermine, of DFMO-injected and PBS-injected fish relative to the
 639 simultaneous controls at 6 h to 7 d post-transfer to 5 ppt or 0.1 ppt water (nmol/g gill).
 640

	5ppt-PBS	5ppt-DFMO	0.1ppt-PBS	0.1ppt-DFMO	<i>F</i>	<i>P</i>
6 h	76.14±2.08	52.13±1.99*	94.25±10.89	63.54±2.41 ^{Δ□}	9.981	0.005
1 d	73.13±2.56	44.13±1.70*	119.05±3.07 ^{&}	60.50±4.98 ^{Δ□}	94.815	<0.001
3 d	75.56±2.74	46.53±5.91*	110.95±10.45 ^{&}	50.18±4.08 ^{Δ□}	20.995	0.001
7 d	75.32±0.88	20.73±1.17*	97.89±11.71 ^{&}	35.28±2.49 ^{Δ□}	3.421	<0.001
<i>F</i>	3.339	4.275	3.837	20.811		
<i>P</i>	0.846	<0.001	0.038	<0.001		

641
 642 **P*<0.05 compared to the 5ppt-PBS injection (sham control) for that time point, ^Δ *P*<0.05
 643 compared to the 0.1ppt PBS injection group for that time point; [&] *P*<0.05 compared to the 5ppt-
 644 PBS injection group for that time point; [□] *P*<0.05 compared to the 5ppt-PBS injection group for
 645 that time point

646 **Fig. 1.** Plasma osmolality ($n = 6$) in *F. grandis* acclimated to 5 ppt water then sampled at pre-
647 transfer or at 6 h, 1 d, 3 d, and 7 d following acute transfer to 0.1, 0.5, 1, 2, and 5 ppt water. The
648 vertical dashed line divides pre-transfer and post-transfer time points. Data represent the mean \pm
649 SEM, mOsM/kg Asterisks indicate a significant difference ($P \leq 0.05$) in comparison to the 5 ppt
650 treatment for that time point; different letters indicate a significant difference ($P \leq 0.05$) in
651 comparison to the pre-transfer for a given salinity.

652
653 **Fig. 2.** Representative scanning electron micrographs of the afferent filamental epithelium of *F.*
654 *grandis* gills after acclimation to 5 ppt and acute transfer to 0.1, 0.5, 1, 2, or 5 ppt water at 6 h, 1
655 d, 3 d, and 7 d post-transfer. Asterisks indicate pavement cells, solid white arrows point to
656 seawater-type mitochondrion-rich cells (MRCs), and dashed white arrows point to freshwater-
657 type MRCs. Scale bar = 5 μm .

658
659 **Fig. 3.** Relative *arg II* and *odc* mRNA levels in mitochondrion-rich cells (MRCs) and pavement
660 cells (PVCs) in gills of fish acclimated to 5 ppt, then acutely transferred to 5 ppt or 0.1 ppt water
661 for 1 d. The mRNA levels were normalized to the mean value of expression in PVCs from 5 ppt-
662 acclimated fish. Data represent the mean \pm SEM ($n = 6$). Different letters indicate a significant
663 difference ($P \leq 0.05$) in comparison to the 5 ppt treatment for the same cell type; asterisks indicate
664 a significant difference ($P \leq 0.05$) in comparison to PVCs for that salinity.

665
666 **Fig. 4.** Plasma osmolality (mOsM/kg) (A), plasma sodium concentration (mM) (B), and plasma
667 chloride concentration (mM) (C) in *F. grandis* acclimated to 5 ppt and sampled at pre-transfer or
668 at 6 h, 1 d, 3 d, and 7 d following acute transfer to 0.1 ppt or 5 ppt water. Fish received
669 intraperitoneal injections of DFMO or PBS (sham control) (*see text for details*). The vertical
670 dashed line divides pre-transfer and post-transfer. Data represent the mean \pm SEM ($n = 6$).
671 Asterisks indicate a significant difference ($P \leq 0.05$) in comparison to the 5 ppt PBS treatment for
672 that time point; letters indicate a significant difference ($P \leq 0.05$) in comparison to the pre-
673 treatment for a given salinity.

674
675 **Fig. 5.** Relative *c-fos* (A) and *c-myc* (B) mRNA levels (relative to the pre-transfer levels), and
676 caspase-3 activity without DFMO application (C) and with DFMO application (D). The vertical

677 dashed line divides pre-transfer and post-transfer. Data represent the mean \pm SEM (n =6).
678 Asterisks indicate significant differences ($P\leq 0.05$) in comparison to the 5 ppt PBS treatment for
679 that time point; letters indicate a significant difference ($P\leq 0.05$) in comparison to the pre-
680 treatment for different time points.

681

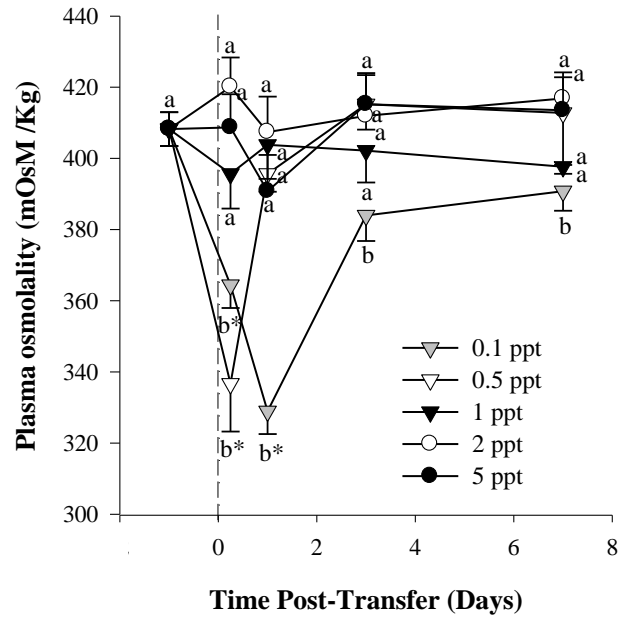
682 **Fig. 6.** Percent change (relative to baseline isotonic conditions) in the short circuit current, I_{sc} (A)
683 and membrane conductance, G_t (B) of opercular epithelia kept in symmetrical conditions to
684 isotonic (Iso) (n =10) or hypotonic (Hypo) solutions (n =10). The vertical dashed line represents
685 the transfer between these two media. Controls represent those epithelia receiving no
686 administration of the polyamine mixture. Asterisks represent significant differences from
687 hypotonic control exposures at the same time points ($P\leq 0.05$). A polyamine mixture (0.4 mM
688 putrescine, 0.3 mM spermidine, and 0.1 mM spermine) was added to the basolateral side of
689 opercular epithelium, either a) coincident with transfer from isotonic to hypotonic conditions
690 (pre-PA), or b) following initial hypotonic transfer and establishment of a steady-state I_{sc} under
691 hypotonic conditions (post-PA).

692

693 **Fig. 7.** Percent change (relative to baseline isotonic conditions) in short circuit current, I_{sc} (A)
694 and membrane conductance, G_t (B) of the opercular epithelium in isotonic (Iso) or hypotonic
695 (Hypo) solutions. The vertical dashed line represents the transfer between these two media.
696 Controls represent those epithelia receiving no addition of polyamines. Data represent the mean
697 \pm SEM (n =6). Single asterisks represent significant differences from hypotonic challenges at the
698 same time points ($P\leq 0.05$); double asterisks represent significant differences from hypotonic
699 challenges at the same time points ($P\leq 0.01$).

700

701



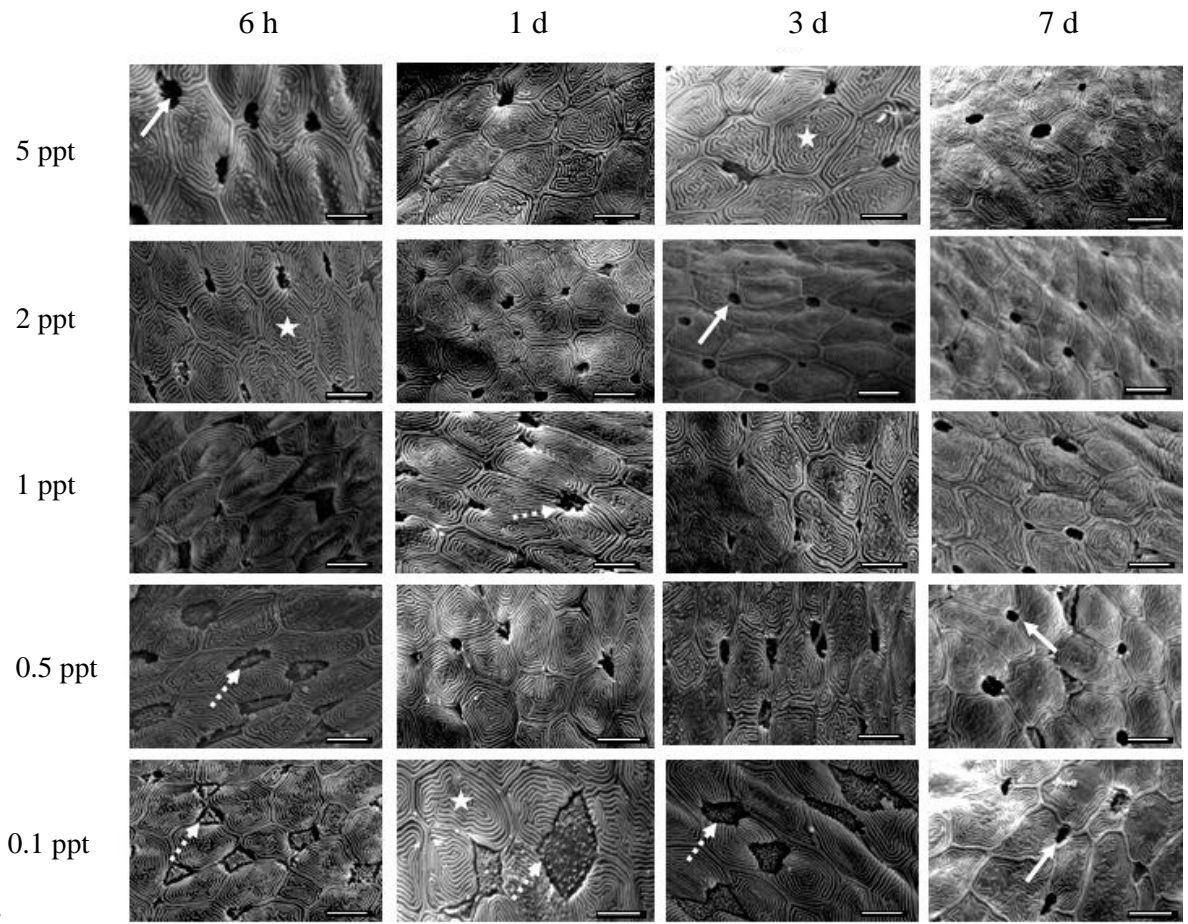
702

703

704 Fig.1

705

706

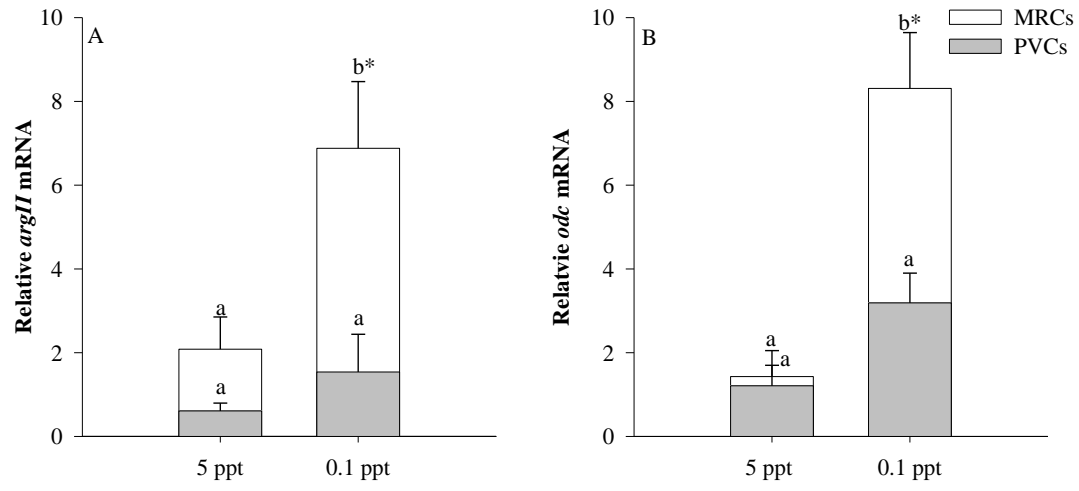


707

708 Fig.2

709

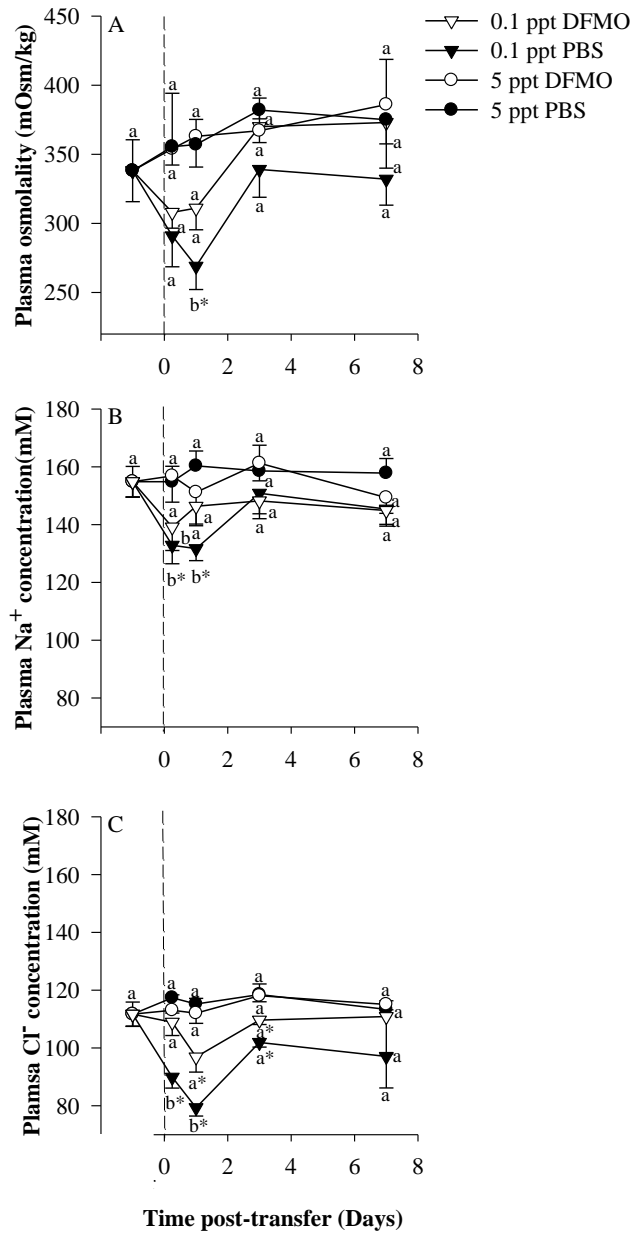
710



711

712 Fig.3

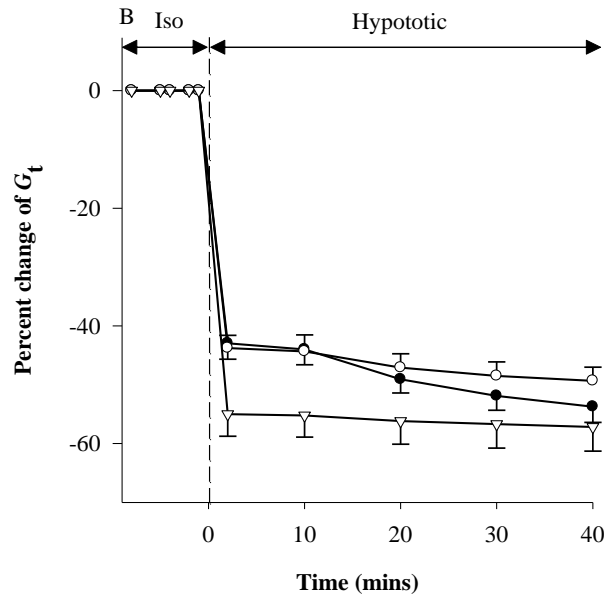
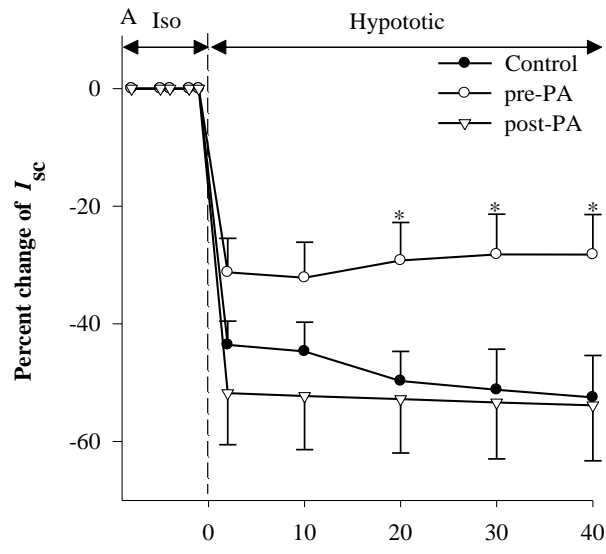
713

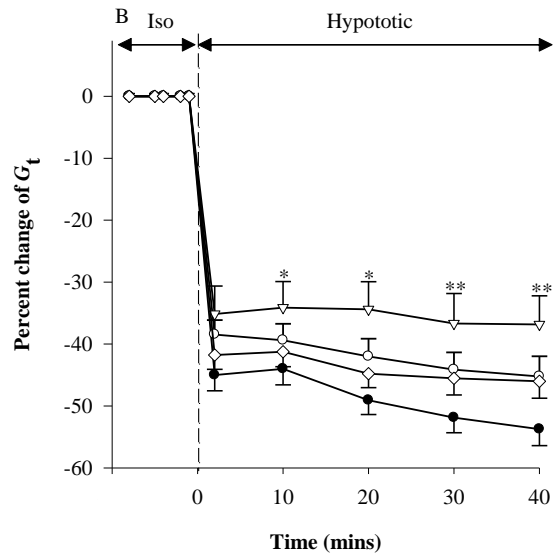
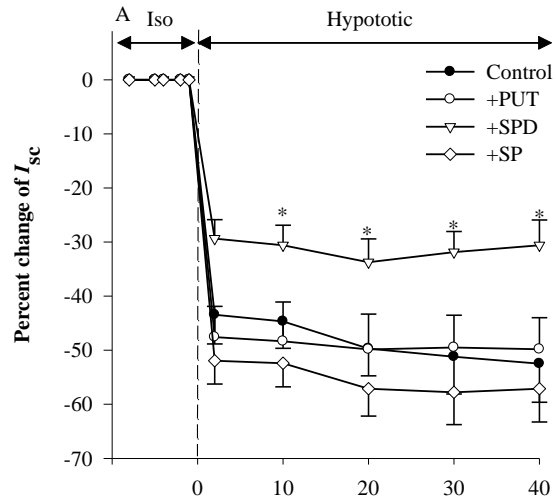


714

715

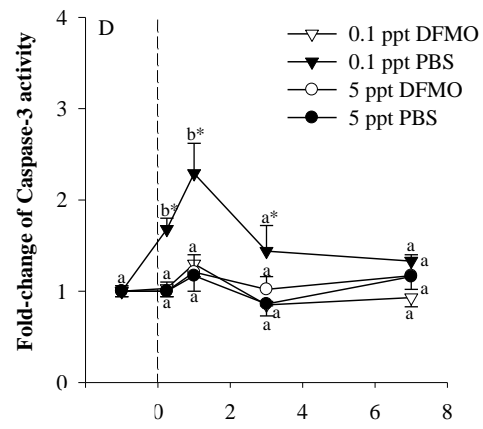
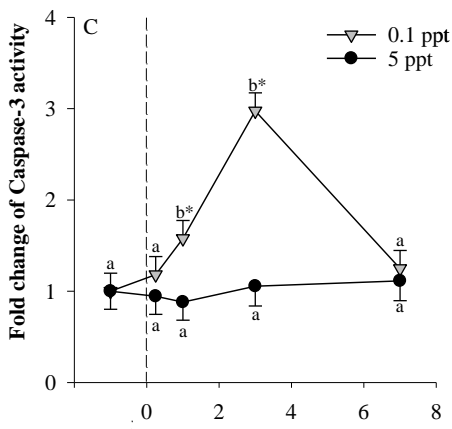
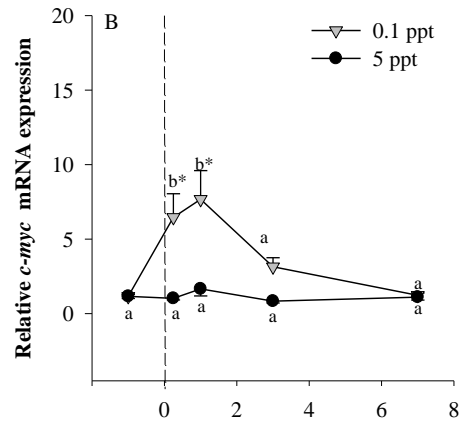
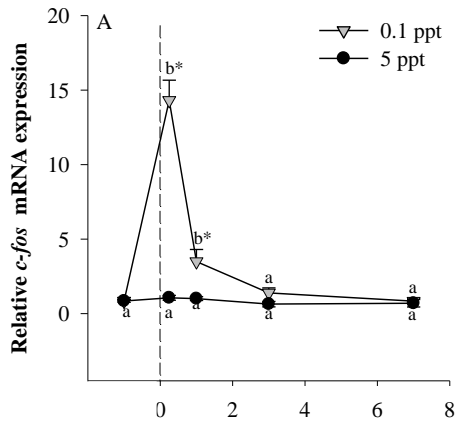
716 Fig.4





720

721 Fig.6



722

Time Post-Transfer (Days)

723 Fig.7

724 **References:**

- 725 Brennan, R.S., Galvez, F., Whitehead, A., 2015. Reciprocal osmotic challenges reveal mechanisms of
726 divergence in phenotypic plasticity in the killifish *Fundulus heteroclitus*. *J. Exp. Biol.* 218, 1212-
727 1222.
- 728 Burnett, K.G., Bain, L.J., Baldwin, W.S., Callard, G.V., Cohen, S., Di Giulio, R.T., Evans, D.H., Gomez-
729 Chiari, M., Hahn, M.E., Hoover, C.A., Karchner, S.I., Katoh, F., MacLatchy, D.L., Marshall, W.S.,
730 Meyer, J.N., Nacci, D.E., Oleksiak, M.F., Rees, B.B., Singer, T.D., Stegeman, J.J., Towle, D.W., Van
731 Veld, P.A., Vogelbein, W.K., Whitehead, A., Winn, R.N., Crawford, D.L., 2007. *Fundulus* as the
732 premier teleost model in environmental biology: Opportunities for new insights using genomics.
733 *Comp. Biochem. Physiol. D* 2, 257-286.
- 734 Cheng, S.X., Geibel, J.P., Hebert, S.C., 2004. Extracellular polyamines regulate fluid secretion in rat
735 colonic crypts via the extracellular calcium-sensing receptor. *Gastroenterology* 126, 148-158.
- 736 Copeland, D.E., 1950. Adaptive behaviour of the chloride cell in the gill of *Fundulus heteroclitus*. *J.*
737 *Morphol.* 87, 369-379.
- 738 Daborn, K., Cozzi, R.R.F., Marshall, W.S., 2001. Dynamics of pavement cell-chloride cell interactions
739 during abrupt salinity change in *Fundulus heteroclitus*. *J. Exp. Biol.* 204, 1889-1899.
- 740 Deng, W., Viar, M.J., Johnson, L.R., 2005. Polyamine depletion inhibits irradiation-induced apoptosis in
741 intestinal epithelia. *Am. J. Physiol.- Gastro Liver Physiol.* 289, G599-606.
- 742 Evans, D.H., Piermarini, P.M., Choe, K.P., 2005. The multifunctional fish gill: Dominant site of gas
743 exchange, osmoregulation, acid-base regulation, and excretion of nitrogenous waste. *Physiol. Rev.* 85,
744 97-177.
- 745 Fleige, S., Walf, V., Huch, S., Prgomet, C., Sehm, J., Pfaffl, M.W., 2006. Comparison of relative mRNA
746 quantification models and the impact of RNA integrity in quantitative real-time RT-PCR. *Biotechnol.*
747 *Letters* 28, 1601-1613.
- 748 Galvez, F., Reid, S.D., Hawkings, G., Goss, G.G., 2002. Isolation and characterization of mitochondria-
749 rich cell types from the gill of freshwater rainbow trout. *Am. J. Physiol. Reg. I.* 282, R658-668.
- 750 Goss, G.G., Laurent, P., Perry, S.F., 1994. Gill morphology during hypercapnia in brown bullhead
751 (*Ictalurus nebulosus*)- role of chloride cells and pavement cells in acid base regulation. *J. Fish Biol.*
752 45, 705-718.
- 753 Griffith, R.W., 1974. Environment and salinity tolerance in the Genus *Fundulus*. *Copeia* 319-331.
- 754 Gu, J., Law, A.Y.S., Yeung, B.H.Y., Wong, C.K.C., 2014. Activation of gill Ca²⁺-sensing receptor as a
755 protective pathway to reduce Ca²⁺-induced cytotoxicity. *J. Mol. Endocrinol.* 53, 155-164.
- 756 Hiroi, J., McCormick, S.D., 2012. New insights into gill ionocyte and ion transporter function in
757 euryhaline and diadromous fish. *Respir. Physiol. Neurobiol.* 184, 257-268.

758 Kaneko, T., Katoh, F., 2004. Functional morphology of chloride cells in killifish *Fundulus heteroclitus*, a
759 euryhaline teleost with seawater preference. *Fisheries Science* 70, 723-733.

760 Karnaky, K.J., Degnan, K.J., Zadunaisky, J.A., 1977. Chloride transport across isolated opercular
761 epithelium of killifish - membrane rich in chloride cells. *Science* 195, 203-205.

762 Katoh, F., Hasegawa, S., Kita, J., Takagi, Y., Kaneko, T., 2001. Distinct seawater and freshwater types of
763 chloride cells in killifish, *Fundulus heteroclitus*. *Can. J. Zool.* 79, 822-829.

764 Katoh, F., Kaneko, T., 2003. Short-term transformation and long-term replacement of branchial chloride
765 cells in killifish transferred from seawater to freshwater, revealed by morphofunctional observations
766 and a newly established 'time-differential double fluorescent staining' technique. *J. Exp. Biol.* 206,
767 4113-4123.

768 Katoh, F., Shimizu, A., Uchida, K., Kaneko, T., 2000. Shift of chloride cell distribution during early life
769 stages in seawater-adapted killifish, *Fundulus heteroclitus*. *Zool. Sci.* 17, 11-18.

770 Kelly, S.P., Fletcher, M., Part, P., Wood, C.M., 2000. Procedures for the preparation and culture of
771 'reconstructed' rainbow trout branchial epithelia. *Methods Cell Sci.* 22, 153-163.

772 Kidder, G.W., Petersen, C.W., Preston, R.L., 2006. Energetics of osmoregulation: II. Water flux and
773 osmoregulatory work in the euryhaline fish, *Fundulus heteroclitus*. *J. Exp. Zool. A Comp. Exp.*
774 *Biol.* 305, 318-327.

775 Krumschnabel, G., Podrabsky, J.E., 2009. Fish as model systems for the study of vertebrate apoptosis.
776 *Apoptosis* 14, 1-21.

777 Laurent, P., Chevalier, C., Wood, C.M., 2006. Appearance of cuboidal cells in relation to salinity in gills
778 of *Fundulus heteroclitus*, a species exhibiting branchial Na⁺ but not Cl⁻ uptake in freshwater. *Cell*
779 *Tissue Res.* 325, 481-492.

780 Lee, K.C., Goh, W.L.P., Xu, M., Kua, N., Lunny, D., Wong, J.S., Coomber, D., Vojtesek, B., Lane, E.B.,
781 Lane, D.P., 2008. Detection of the p53 response in zebrafish embryos using new monoclonal
782 antibodies. *Oncogene* 27, 629-640.

783 Loretz, C.A., 2008. Extracellular calcium-sensing receptors in fishes. *Comp. Biochem. Physiol. A* 149,
784 225-245.

785 Lu, G., Mak, Y.T., Wai, S.M., Kwong, W.H., Fang, M.R., James, A., Randall, D., Yew, D.T., 2005.
786 Hypoxia-induced differential apoptosis in the central nervous system of the sturgeon (*Acipenser*
787 *shrenckii*). *Microsc. Res. Tech.* 68, 258-263.

788 Marshall, W.S., 2003. Rapid regulation of NaCl secretion by estuarine teleost fish: coping strategies for
789 short-duration freshwater exposures. *Biochimica Biophysica Acta- Biomembranes* 1618, 95-105.

790 Marshall, W.S., 2011. Mechanosensitive signalling in fish gill and other ion transporting epithelia. *Acta*
791 *Physiol.* 202, 487-499.

792 Marshall, W.S., Bryson, S.E., 1998. Transport mechanisms of seawater teleost chloride cells: An
793 inclusive model of a multifunctional cell. *Comp. Biochem. Physiol. A* 119, 97-106.

794 Marshall, W.S., Bryson, S.E., Garg, D., 1993. Alpha-2-adrenergic inhibition of Cl⁻ transport by opercular
795 epithelium is mediated by intracellular Ca²⁺. *Proc. Natl. Acad. Sci. U. S. A.* 90, 5504-5508.

796 Marshall, W.S., Bryson, S.E., Luby, T., 2000. Control of epithelial Cl⁻ secretion by basolateral osmolality
797 in the euryhaline teleost *Fundulus heteroclitus*. *J. Exp. Biol.* 203, 1897-1905.

798 Marshall, W.S., Emberley, T.R., Singer, T.D., Bryson, S.E., McCormick, S.D., 1999. Time course of
799 salinity adaptation in a strongly euryhaline estuarine teleost, *Fundulus heteroclitus*: a multivariable
800 approach. *J. Exp. Biol.* 202, 1535-1544.

801 Marshall, W.S., Grosell, M., 2005. Ion transport, osmoregulation, and acid-base balance, in: D.H. Evans,
802 J.B. Claiborne (Eds.), *Physiology of Fishes*. CRC Press, Boca Raton, FL, 177-230.

803 Marshall, W.S., Ossum, C.G., Hoffmann, E.K., 2005. Hypotonic shock mediation by p38 MAPK, JNK,
804 PKC, FAK, OSR1 and SPAK in osmosensing chloride secreting cells of killifish opercular epithelium.
805 *J. Exp. Biol.* 208, 1063-1077.

806 Morris, S.M., Jr, 2004. Enzymes of arginine metabolism. *J. Nutr.* 134, S2743-2747.

807 Muscari, C., Bonafe, F., Stanic, I., Flamigni, F., Stefanelli, C., Farruggia, G., Guarnieri, C., Caldarera,
808 C.M., 2005. Polyamine depletion reduces TNFalpha/MG132-induced apoptosis in bone marrow
809 stromal cells. *Stem Cells* 23, 983-991.

810 Patrick, M.L., Wood, C.M., Marshall, W.S., 1997. Calcium regulation in the freshwater-adapted
811 *mummichog*. *J. Fish Biol.* 51, 135-145.

812 Pegg, A.E., McCann, P.P., 1982. Polyamine metabolism and function. *Am. J. Physiol. Cell Ph.* 243,
813 C212-221.

814 Perry, S.F., Goss, G.G., Fenwick, J.C., 1992. Interrelationships between gill chloride cell morphology and
815 calcium uptake in freshwater teleosts. *Fish Physiol. Biochem.* 10, 327-337.

816 Peter, H.W., Ahlers, J., Gunther, T., 1978. Dependence of polyamine and phospholipid contents in
817 marine-bacteria on osmotic strength of medium. *Int. J. Biochem.* 9, 313-316.

818 Poulin, R., Wechter, R.S., Pegg, A.E., 1991. An early enlargement of the putrescine pool is required for
819 growth in L1210 mouse leukemia cells under hypoosmotic stress. *J. Biol. Chem.* 266, 6142-6151.

820 Quinn, S.J., Ye, C.P., Diaz, R., Kifor, O., Bai, M., Vassilev, P., Brown, E., 1997. The Ca²⁺-sensing
821 receptor: a target for polyamines. *Am. J. Physiol. Cell Physiol.* 273, C1315-1323.

822 Ray, R.M., Viar, M.J., Yuan, Q., Johnson, L.R., 2000. Polyamine depletion delays apoptosis of rat
823 intestinal epithelial cells. *Am. J. Physiol. Cell Physiol.* 278, 480-489.

824 Ray, R.M., Zimmerman, B.J., McCormack, S.A., Patel, T.B., Johnson, L.R., 1999. Polyamine depletion
825 arrests cell cycle and induces inhibitors p21(Waf1/Cip1), p27(Kip1), and p53 in IEC-6 cells. *Am. J.*
826 *Physiol. Cell Physiol.* 276, C684-691.

827 Reis, M.I.R., Nascimento, D.S., do Vale, A., Silva, M.T., dos Santos, N.M.S., 2007. Molecular cloning
828 and characterisation of sea bass (*Dicentrarchus labrax* L.) caspase-3 gene. *Mol. Immunol.* 44, 774-
829 783.

830 Rojo, C., Gonzalez, E., 1999. Ontogeny and apoptosis of chloride cells in the gill epithelium of newly
831 hatched rainbow trout. *Acta Zoologica* 80, 11-23.

832 Scott, G.R., Baker, D.W., Schulte, P.M., Wood, C.M., 2008. Physiological and molecular mechanisms of
833 osmoregulatory plasticity in killifish after seawater transfer. *J. Exp. Biol.* 211, 2450-2459.

834 Scott, G.R., Rogers, J.T., Richards, J.G., Wood, C.A., Schulte, P.M., 2004. Intraspecific divergence of
835 ionoregulatory physiology in the euryhaline teleost *Fundulus heteroclitus*: possible mechanisms of
836 freshwater adaptation. *J. Exp. Biol.* 207, 3399-3410.

837 Scott, G.R., Schulte, P.M., 2005. Intraspecific variation in gene expression after seawater transfer in gills
838 of the euryhaline killifish *Fundulus heteroclitus*. *Comp. Biochem. Physiol. A* 141, 176-182.

839 Scott, G.R., Schulte, P.M., Wood, C.M., 2006. Plasticity of osmoregulatory function in the killifish
840 intestine: drinking rates, salt and water transport, and gene expression after freshwater transfer. *J. Exp.*
841 *Biol.* 209, 4040-4050.

842 Tabib, A., Bachrach, U., 1994. Activation of the protooncogene c-myc and c-fos by c-ras involvement of
843 polyamines. *Biochem. Biophys. Res. Commun.* 202, 720-727.

844 Tabor, C.W., Tabor, H., 1984. Polyamines. *Annu. Rev. Biochem.* 53, 749-790.

845 Takle, H., McLeod, A., Andersen, O., 2006. Cloning and characterization of the executioner caspases 3, 6,
846 7 and Hsp70 in hyperthermic Atlantic salmon (*Salmo salar*) embryos. *Comp. Biochem. Physiol. B*
847 144, 188-198.

848 Tantini, B., Fiumana, E., Cetrullo, S., Pignatti, C., Bonavita, F., Shantz, L.M., Giordano, E., Muscari, C.,
849 Flamigni, F., Guarnieri, C., Stefanelli, C., Calderera, C.M., 2006. Involvement of polyamines in
850 apoptosis of cardiac myoblasts in a model of simulated ischemia. *J. Mol. Cell. Cardiol.* 40, 775-782.

851 Uthaiwan, K., Chatchavalvanich, K., Noparatnaraporn, N., Machado, J., 2001. Scanning electron
852 microscopy of glochidia and juveniles of the freshwater mussel, *Hyriopsis myersiana*. *Invertebr.*
853 *Reprod. Dev.* 40, 143-151.

854 Watts, S.A., Yeh, E.W., Henry, R.P., 1996. Hypoosmotic stimulation of ornithine decarboxylase activity
855 in the brine shrimp *Artemia franciscana*. *J. Exp. Zool.* 274, 15-22.

856 Whitehead, A., Galvez, F., Zhang, S.J., Williams, L.M., Oleksiak, M.F., 2011a. Functional genomics of
857 physiological plasticity and local adaptation in killifish. *J. Hered.* 102, 499-511.

858 Whitehead, A., Roach, J.L., Zhang, S., Galvez, F., 2011b. Genomic mechanisms of evolved physiological
859 plasticity in killifish distributed along an environmental salinity gradient. Proc. Natl. Acad. Sci. U. S.
860 A. 108, 6193-6198.

861 Whitehead, A., Roach, J.L., Zhang, S.J., Galvez, F., 2012. Salinity- and population-dependent genome
862 regulatory response during osmotic acclimation in the killifish (*Fundulus heteroclitus*) gill. J. Exp.
863 Biol. 215, 1293-1305.

864 Wongyai, S., Oefner, P., Bonn, G., 1988. HPLC analysis of polyamines and their acetylated derivatives in
865 the picomole range using benzoyl chloride and 3,5-dinitrobenzoyl chloride as derivatizing agent.
866 Biomed. Chromatogr. 2, 254-257.

867 Wood, C.M., Grosell, M., 2008. A critical analysis of transepithelial potential in intact killifish (*Fundulus*
868 *heteroclitus*) subjected to acute and chronic changes in salinity. J. Comp. Physiol. B 178, 713-727.

869 Wood, C.M., Grosell, M., 2009. TEP on the tide in killifish (*Fundulus heteroclitus*): effects of
870 progressively changing salinity and prior acclimation to intermediate or cycling salinity. J. Comp.
871 Physiol. B 179, 459-467.

872 Wood, C.M., LeMoigne, J., 1991. Intracellular acid-base responses to environmental hyperoxia and
873 normoxic recovery in rainbow trout. Resp. Physiol. 86, 91-113.

874 Yamashita, M., Mizusawa, N., Hojo, M., Yabu, T., 2008. Extensive apoptosis and abnormal
875 morphogenesis in pro-caspase-3 transgenic zebrafish during development. J. Exp. Biol. 211, 1874-
876 1881.

877 Zall, D.M., Fisher, D., Garner, M.Q., 1956. Photometric determination of chlorides in water. Anal. Chem.
878 28, 1665-1668.

879 Zapata, P.J., Serrano, M., Pretel, A.T., Amoros, A., Botella, M.A., 2004. Polyamines and ethylene
880 changes during germination of different plant species under salinity. Plant Science 167, 781-788.

881